fire

MDPI

Article

Fire Risk Quantification Assessment and Critical Path Identification Concerning Containerized Mobile Power Supplies in Temporary Port Storage

Zhen Qiao [1,*], Xiaotiao Zhan [1,*], Yao Tian [1], Yuan Gao [1], Longjun He [1], Yamei Zeng [1], Wenhui Chen [1], Yu Meng [1] and Yuechao Zhao [2]

[1] Safety Quality Technology Research Center, China Waterborne Transport Research Institute, Beijing 100088, China; tianyao@wti.ac.cn (Y.T.); gaoyuan@wti.ac.cn (Y.G.); helongjun@wti.ac.cn (L.H.); zengym@wti.ac.cn (Y.Z.); chenwenhui@wti.ac.cn (W.C.); mengyu@wti.ac.cn (Y.M.)
[2] Navigation College, Dalian Maritime University, Dalian 116026, China; aqzyc@dlmu.edu.cn
* Correspondence: qiaozhen@wti.ac.cn (Z.Q.); zhanxiaotiao@wti.ac.cn (X.Z.)

Abstract

Containerized mobile power supplies (CMPS), a critical energy replenishment carrier for all-electric ships, have caused severe economic losses via frequent fire and explosion accidents during temporary port storage in recent years. Existing literature focuses on battery thermal runaway under laboratory conditions and maritime transport risk analysis, but its conclusions are not directly applicable to port temporary storage. Port storage, featuring full-charge quiescent placement and high turnover, differs significantly from maritime transport, while its high-temperature and humid environment is distinct from laboratory settings. Furthermore, no system safety-based risk assessment framework exists, failing to deliver targeted mitigation strategies for practical operations. To address these issues, fault tree analysis (FTA), Bayesian network (BN), and attack–defense game theory were combined to build a systematic safety risk assessment framework. FTA clarified the hazard factors' correlation mechanism; based on FTA, BN conducted a quantitative evaluation. Extended from BN results, attack–defense game theory identified key risk evolution paths and formulated targeted prevention and control measures. The main conclusions are as follows: Combined with similar accident features and port storage scenario attributes, internal correlations between hazard-inducing factors were clarified via FTA. Based on expert evaluations and BN calculation, the target port's fire accident occurrence probability was determined as 2.41%, with two core root nodes identified via sensitivity analysis. Two critical risk evolution paths corresponding to IE1 (thermal runaway initiation) and IE2 (failure of protection and emergency response systems) were identified via game theory and traversal method, with occurrence probabilities of 1.50% and 1.77%, respectively. Targeted prevention and control measures adapted to the port storage scenario were proposed based on path triggering mechanisms. These findings provide theoretical support for port enterprises to improve CMPS fire prevention and emergency response capabilities, elevate port safety management levels, and promote the safe development of the all-electric vessel shipping industry.

Keywords: containerized mobile power supply; temporary port storage; fire accident; risk analysis; quantitative assessment

Check for updates

Academic Editor: Depeng Kong

Received: 9 April 2026
Revised: 13 May 2026
Accepted: 15 May 2026
Published: 17 May 2026

Copyright: © 2026 by the authors. Licensee MDPI, Basel, Switzerland. This article is an open access article distributed under the terms and conditions of the Creative Commons Attribution (CC BY) license.

1. Introduction

With the growing prominence of global climate challenges, all-electric ships, with their inherent low-carbon and eco-friendly attributes, have emerged as a core pathway for the low-carbon transition of the global shipping industry [1–3]. Containerized mobile power supplies, as the mainstream power replenishment unit for all-electric vessels [4,5], are predominantly equipped with lithium iron phosphate (LFP) batteries; upon berthing, vessels complete energy replenishment by hoisting full state-of-charge (SOC) units stored in port yards [6]. In 2025, a container fire and explosion at the Port of Los Angeles destroyed over a hundred containers and forced a complete halt to port operations. A subsequent container blaze at Pakistan's Port of Karachi in 2026 gutted 20 containers and suspended terminal activities for more than 48 h. These two high-profile port incidents starkly expose grave safety risks that lurk in the temporary yard stacking of fully charged energy storage devices at container terminals. Stored as temporary transit goods in port terminals, such equipment remains in a full-SOC static state with a rapid turnover cycle; coupling fluctuating open-air port environments with dynamic loading from hoisting operations further exacerbates fire hazards. Consequently, this necessitates targeted research on the fire risk of mobile batteries specific to this distinct storage scenario.

LFP thermal runaway behavior constitutes a critical trigger for fire and explosion incidents. The prevailing IMDG Code Amendment 42-24 released by the International Maritime Organization, together with China's industrial standard JT/T 1543-2025 [7] issued by the Ministry of Transport, sets out regulatory constraints for containerized mobile power supplies classified as cargo. In contrast, marine power installations are categorized as shipborne auxiliary facilities and are not managed as cargo during temporary port storage. Within academic circles, existing research predominantly centers on the intrinsic thermal runaway (TR) properties. For instance, Meng et al. [8] featured the surface temperature threshold for TR triggering at 166.8 °C. Zhou et al. [9] further demonstrated that increasing the heating process exponentially shortens the TR onset time of full-SOC cells. Regarding the impact of cyclic aging on the full-SOC LFP batteries, Wang et al. [10] revealed that cells cycled at a 4C rate still pose an important TR propagation risk within a 1 m range; Frivaldsky et al. [11] elucidated the mechanism underlying the effects of charge–discharge cycling on the electrochemical performance of cells. For marine-specific energy storage scenarios, Wang et al. [12] investigated the influence of TR initiation in the middle layer of a three-tier marine battery cabinet on upper and lower battery layers, as well as the associated in-pack TR propagation behavior. From a monitoring and early-warning perspective, Jin et al. [13] developed a rapid early TR detection scheme based on swelling force. Zhang et al. [14] identified the explosion characteristics of TR-released combustible gases via numerical simulation. In addition, Schoberl et al. [15], Shareef et al. [16], and Li et al. [17] explored technical pathways to mitigate lithium battery TR hazards from a material design standpoint.

Moreover, scholars have conducted targeted research into the risk analysis of the containerized mobile power supply. Liu et al. [5] proposed a risk analysis framework integrating fuzzy evidence reasoning and a dynamic network algorithm, identifying the two highest-priority failure modes as lightning protection system failure and loading–unloading operating malfunction. Yang et al. [18] adopted a fuzzy fault tree analysis model based on grounded theory, confirming that battery quality defects and condition monitoring equipment failure are the primary causes of fire accidents. Yin et al. [19] systematically summarized three core risk categories faced by marine lithium batteries, namely mechanical, electrical, and thermal abuse, and clarified the key factors inducing battery failure. Focusing on the safety protection of marine energy storage systems, Lee et al. [20] developed an artificial intelligence-based fault prediction algorithm. Guo et al. [21] established a real-time

risk monitoring method for battery systems based on risk index date, enabling accurate diagnosis of battery aging and abnormal cells.

Overall, existing studies have yielded relatively substantial findings in two core areas: the thermal runaway features of lithium iron phosphate batteries and the risk analysis of containerized mobile power supply.

However, most of the available research centers on standard laboratory operating conditions or ship navigation scenarios. While they yield key thermal runaway parameters for fully charged batteries and identify core risk factors in ship navigation, they diverge substantially from the port temporary stacking scenario targeted in this study. First, port temporary stacking features rapid turnover and is not regulated under conventional dangerous goods storage criteria. The local high-temperature and high-humidity environment contrasts sharply with standard laboratory settings, and its fast turnover mechanism also differs from ship navigation operations. Second, existing fire risk assessments mostly concentrate on the intrinsic thermal runaway properties of batteries, with few efforts probing multi-factor coupling risks from a system safety perspective.

Accordingly, this study integrated fault tree analysis (FTA), Bayesian network (BN), and attack–defense game theory to investigate systematic safety risks in view of the operational attributes of temporary port storage. Drawing on documented accident cases and the operational conditions concerning the target port, the research adopted FTA to qualitatively identify hazard factors and their interrelationships. Then, it employed BN to quantify risk probability and incorporated attack–defense game theory to delineate core risk evolution paths, on the basis of which optimized prevention and control measures were proposed. To fulfill those research objectives, the study was structured around establishing a multi-theoretical evaluation system, dissecting hazard-inducing chains, implementing quantitative risk characterization, identifying critical paths, and formulating targeted management strategies. The findings of this study can provide theoretical support and practical countermeasures for port enterprises to standardize the temporary storage management and prevent similar fire accidents.

2. Methods

The research logic of this paper, as displayed in Figure 1, was divided into three levels: identification of hazard-inducing factors, quantitative risk analysis, and risk assessment and control, ultimately completing the safety analysis of fire accidents involving marine containerized mobile power supplies in temporary port storage. Special emphasis was placed on quantitative risk analysis, which adopted a multi-model evaluation system incorporating FTA, BN, and offense–defense game theory. Specifically, FTA clarified the internal logic of hazard-inducing factors and provided a logical framework for subsequent quantitative calculations; BN performed quantitative assessment based on the clarified internal logic; the offense–defense game theory was further expanded on the basis of Bayesian analysis to identify key risk paths and propose targeted prevention and control strategies. These three methods were closely linked and progressively advanced, forming a complete research chain from qualitative identification, quantitative assessment, and engineering application guidance. The specific research process was refined into four implementation steps.

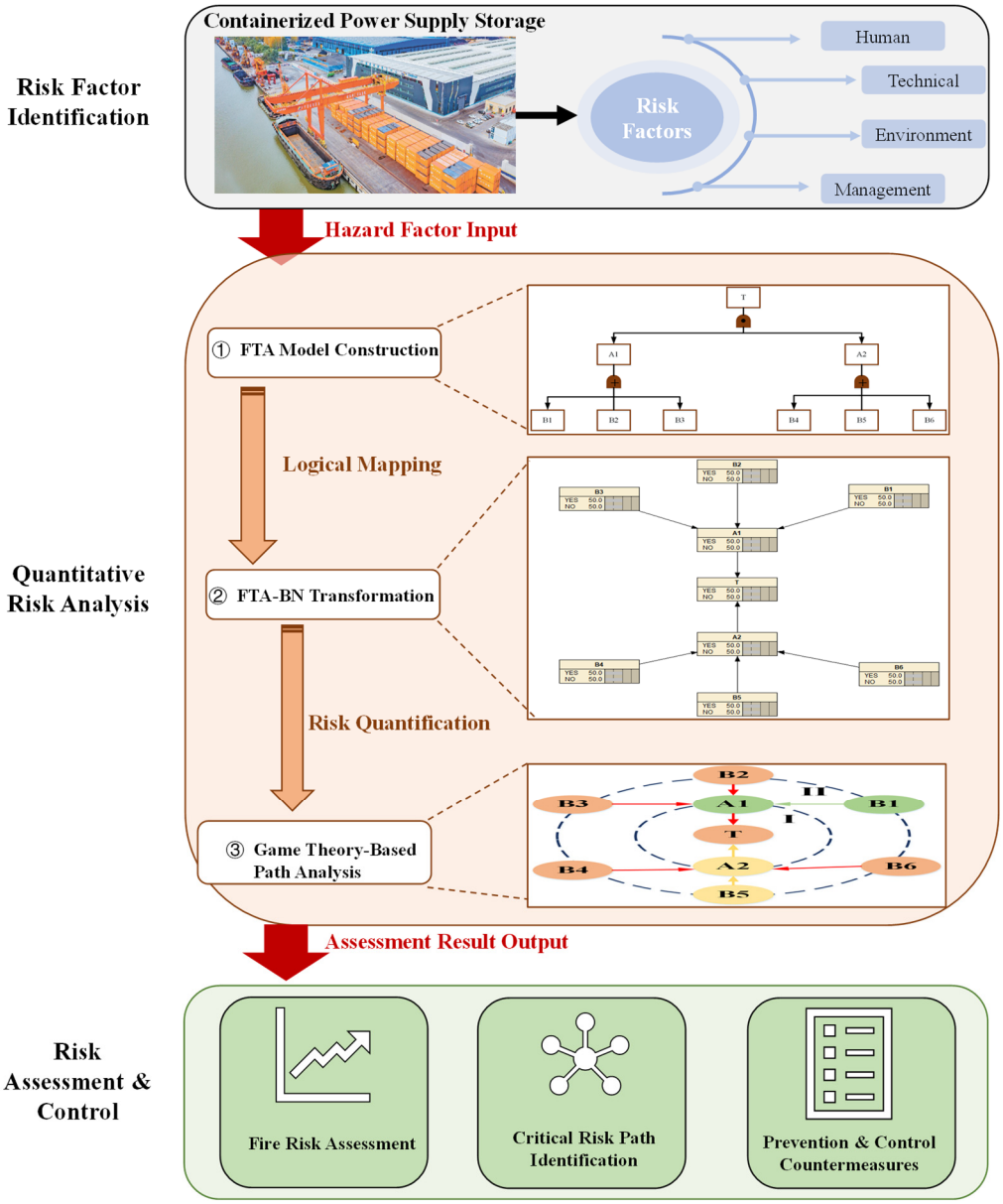


Figure 1. Methodology and research approach.

Step 1: Hazard-inducing factor identification

The whole process of temporary port storage for containerized mobile power supplies was set as the research context, and publicly accessible investigation records of similar fire incidents were systematically collated. All adopted cases were sourced from official accident reports released by national governments, maritime regulatory authorities, and the International Maritime Organization. This work was conducted from four dimensions: personnel, equipment, environment, and management. Three core scenario-specific characteristics were covered in the identification process: first, the equipment perspective, the intrinsic risk of battery cells at full state of charge; second, the environment perspective, the effects of a high-humidity, high-salinity environment at port terminals; third, the management perspective, safety control loopholes in temporary storage operations. Specific details of the cited accident cases were elaborated in Section 3.

Step 2: Qualitative analysis via FTA

FTA is a classic causal analysis method in the field of safety engineering [22–24]. The causal relationship between the top event and underlying hazard-inducing factors was clearly mapped through its hierarchical logic gate structure. The fire accident during containerized mobile power supply storage was set as the top event, and the identified hazard-inducing factors were defined as basic events, after which intermediate event layers were constructed according to causal logic to finalize the FTA model. Scattered risk elements were converted into a visual causal chain in this step. The internal correlation between each hazard-inducing factor was clarified, and the qualitative risk assessment was completed. It should be noted that documented cases of similar fire incidents were relatively scarce. To ensure the comprehensiveness of hazard-inducing factor identification and the rationality of the logical framework for FTA, a total of 20 industry experts were organized for professional argumentation. The panel comprised 5 front-line operators, 5 on-site managers of port enterprises, 5 port safety supervisors, and 5 researchers from universities and research institutes, which guaranteed the overall reliability of the research findings.

Step 3: Quantitative calculation via BN

BN is a graphical model based on probabilistic reasoning. The dependency between variables is characterized through a directed acyclic graph, and forward probability calculation and reverse reasoning under uncertain information are completed with the conditional probability table (CPT) [25–27]. Taking the causal logic structured by FTA as the basic framework, FTA event nodes were mapped to BN network modes following standard conversion rules, and logic gate relationships were converted into directed edges and CPTs of the network to realize the effective integration of the two models. After the BN model was established, industry experts and researchers were invited to assign occurrence probabilities to each basic event using the Delphi method. The quantitative calculation of the fire occurrence probability of the top event was realized through this process. Data analysis for BN was performed using Netica 5.18. This tool was well suited for complex modeling scenarios with coupled multiple hazard factors and enabled forward inference and backward diagnostic reasoning, conforming to the demands of risk identification and deduction. In terms of computational accuracy, it integrated a built-in efficient evidence propagation engine that supported up to five significant figures in probabilistic calculation. Characterized by stable operation and high computational precision, it satisfied the accuracy specifications of quantitative risk assessment.

Step 4: Critical risk evolution path identification

Attack–defense game theory is based on a non-cooperative game framework. With Nash equilibrium as the core principle, the optimal attack path and optimal defense path are solved through strategy matching between two game parties [28–30]. The application of attack–defense game theory acted as a further extension of BN calculation results. Sensitivity analysis with BN pinpointed key hazard-inducing factors, but could not quantify the occurrence probability of accident chains containing such factors. The attacker and defender paradigms in the game theory matched FTA causal chains and port preventive strategies. Outcomes of their dynamic games reflected the occurrence probability of each causal factor as well as their internal correlation characteristics. With this concept, the traversal method was employed to compute all potential risk evolution paths in BN and determine the probability of each path inducing the top event. Critical risk evolution paths were filtered via comparative probability analysis. The method delineated complete risk evolution chains and enabled quantitative estimation of the occurrence probability for each path simultaneously.

3. Results

Hazard-inducing factor identification was based on typical accidents in recent years. The statistical results of the identification work are presented in Table 1, covering all publicly available accident cases related to containerized mobile power supply. Mobile power was integrated with a Battery Management System (BMS), Energy Management System (EMS), and supporting monitoring systems. While these systems enhanced the management and control capability of battery states, they also increased the complexity of electrical circuits and elevated the occurrence probability of electrical malfunctions.

Table 1. Statistics of fire and explosion accidents of containerized mobile power supplies in the past three years.

Time	Location	Event	Loss	Cause
16 January 2026	Karachi Port Terminal Yard, Pakistan	Fire accident	20 containers burned down, operation interruption for more than 48 h	(1) TR of full SOC batteries (2) Deficiency in storage management and control
21 November 2025	Yusen Terminal, Port of Los Angeles, USA	Fire and explosion accident	More than 100 containers damaged, port operation interrupted	(1) TR caused by electrical malfunction (2) Absence of special management and control for storage
9 August 2024	Beilun Terminal, Ningbo Zhoushan Port, Zhejiang, China	Deflagration accident	Direct economic loss of 13 million USD	Hazardous chemicals ignited by TR
25 December 2023	"Genius Star XI", USA	Fire accident	41 sets of battery units damaged, with a loss of 3.8 million USD	(1) Securing failure during port container loading (2) TR caused by collision

The fire and explosion accident at the Port of Los Angeles, USA, on 21 November 2025, was directly triggered by battery thermal runaway induced by an electrical malfunction. The fire accident at the Port of Karachi, Pakistan, on 16 January 2026, led to the complete burnout of 20 shipping containers, which was caused by the intrinsic risk of full-SOC batteries coupled with the lack of targeted management and control in the storage process. One additional typical marine accident was included in the analysis. The fire accident on the US vessel "Genius Star XI" on 25 December 2023, was caused by mechanical damage from a transportation collision, which originated from battery securing failure during port container loading and eventually triggered thermal runaway.

Hazard-inducing factors were identified based on risk features exposed by accident cases, combined with the TR of lithium batteries, structural characteristics of containerized mobile power supply, and scenario features of temporary port storage. The internal logic of factors was visually characterized via FTA, with corresponding results presented in Table 2 and Figure 2A.

In the established FTA model, the fire accident was set as the top event. This top event was linked through an AND gate to two intermediate events: thermal runaway initiation and failure of protection and emergency response systems. A fire accident would only occur when both intermediate events took place simultaneously. Thermal runaway initiation covered three verified main causes from accident cases: mechanical damage, electrical short circuit, and heat accumulation, with supplementary triggering paths of external incentives specific to port yard scenarios. The failure of protection and emergency response systems

was analyzed from three core dimensions: built-in fire protection systems, external fire protection support, and on-site emergency disposal capacity.

Table 2. Classification of fire accident hazard-inducing factors.

Symbol	Meaning	Symbol	Meaning	Symbol	Meaning
A1	Thermal runaway initiation	A2	Failure of protection and emergency response systems	B1	Mechanical damage-induced initiation
B2	Electrical short-circuit-induced initiation	B3	Thermal accumulation-induced initiation	B4	External incentive-induced initiation
B5	Failure of built-in fire protection systems	B6	Failure of external fire protection support systems	B7	Failure of emergency response capability
C1	Dynamic load-induced damage	C2	Damage–corrosion coupling-induced initiation	C3	Insulation breakdown and leakage caused by high-humidity salt spray
C4	Loosening of high-voltage connectors and arc discharge induced by vibration	C5	Inductive overvoltage breakdown caused by unconnected lightning protection grounding in the storage area	C6	Electromagnetic interference caused by irregular temporary power wiring
C7	Insulation abrasion and short circuit caused by improper cable laying	C8	Excessive thermal input	C9	Heat dissipation failure
C10	Risk amplification due to lack of protective measures	C11	VOC gas ignition by sparks from hot work in adjacent areas	C12	Local thermal runaway induced by contact with high-temperature work residues
C13	Thermal runaway spread from adjacent box-type power supplies	C14	VOC accumulation and ignition caused by power failure of emergency exhaust systems	C15	Detection-triggering failure
C16	Failure of fire extinguishing medium and redundancy systems	C17	Defects in fire protection system configuration	C18	Lack of operational conditions for fire fighting
C19	Absence of special emergency plans for temporary storage	C20	Inadequate mastery of lithium battery fire response skills by operators	C21	No pre-deployment of emergency supplies
C22	No linkage mechanism established with port fire protection departments	C23	Failure of emergency shutdown devices	D1	Diaphragm thinning and stress concentration induced by stacking extrusion
D2	Tab micro-cracking and bracket plastic deformation induced by hoisting impact	D3	Electrode group displacement induced by cabinet resonance caused by wind loads	D4	Local overpressure and diaphragm breakdown caused by uneven ground

Table 2. *Cont.*

Symbol	Meaning	Symbol	Meaning	Symbol	Meaning
D5	Module collision caused by battery rack fixation failure	D6	Protective structure damage induced by mechanical scratching	D7	Salt spray/rainwater intrusion caused by weathertightness failure
D8	Electrochemical corrosion of damaged parts induced by port salt spray	D9	Contact resistance mutation and partial discharge at tabs caused by corrosion products	D10	Ambient thermal input induced by solar radiation and container greenhouse effect
D11	Increased self-discharge heat generation rate of fully charged batteries	D12	Thermal radiation superposition caused by excessive storage density	D13	Horizontal heat dissipation blockage caused by insufficient storage spacing
D14	Vertical heat dissipation blockage caused by excessive stacking height	D15	Ventilation efficiency attenuation caused by port dust clogging vents	D16	Sharp increase in heat conduction caused by damage to cabinet thermal insulation layers
D17	Temperature control system failure due to power outage	D18	BMS failure caused by UPS power supply interruption	D19	BMS balancing function failure with excessive voltage difference between fully charged cells
D20	Overcharging risk caused by EMS failure to cut off the floating charging circuit for fully charged batteries	D21	Monitoring data not transmitted to shore-based systems or unreasonable early-warning thresholds	D22	Temperature/smoke/flammable gas sensor failure or response delay
D23	Defects in the linkage logic between sensors and fire extinguishing systems	D24	Solenoid cylinder valve jamming or excessive activation pressure	D25	Lack of combined temperature and smoke detectors
D26	Heptafluoropropane extinguishing agent leakage resulting in concentration below the 9% design value	D27	Interlock failure of dual redundant fire extinguishing systems	D28	Mismatch between fire extinguishing systems and lithium battery thermal runaway characteristics
D29	Lack of backup extinguishing agent for fire extinguishing systems	D30	No configuration of lithium battery-specific extinguishing agents	D31	Fire hydrants not covering the temporary storage area
D32	Incompatibility between fire-fighting interfaces and port shore-based systems	D33	Fire-fighting access blocked or insufficient in width	D34	Lack of emergency operation platforms affecting fire-fighting operations
D35	Impeded rescue due to absence of toxic gas early-warning systems				

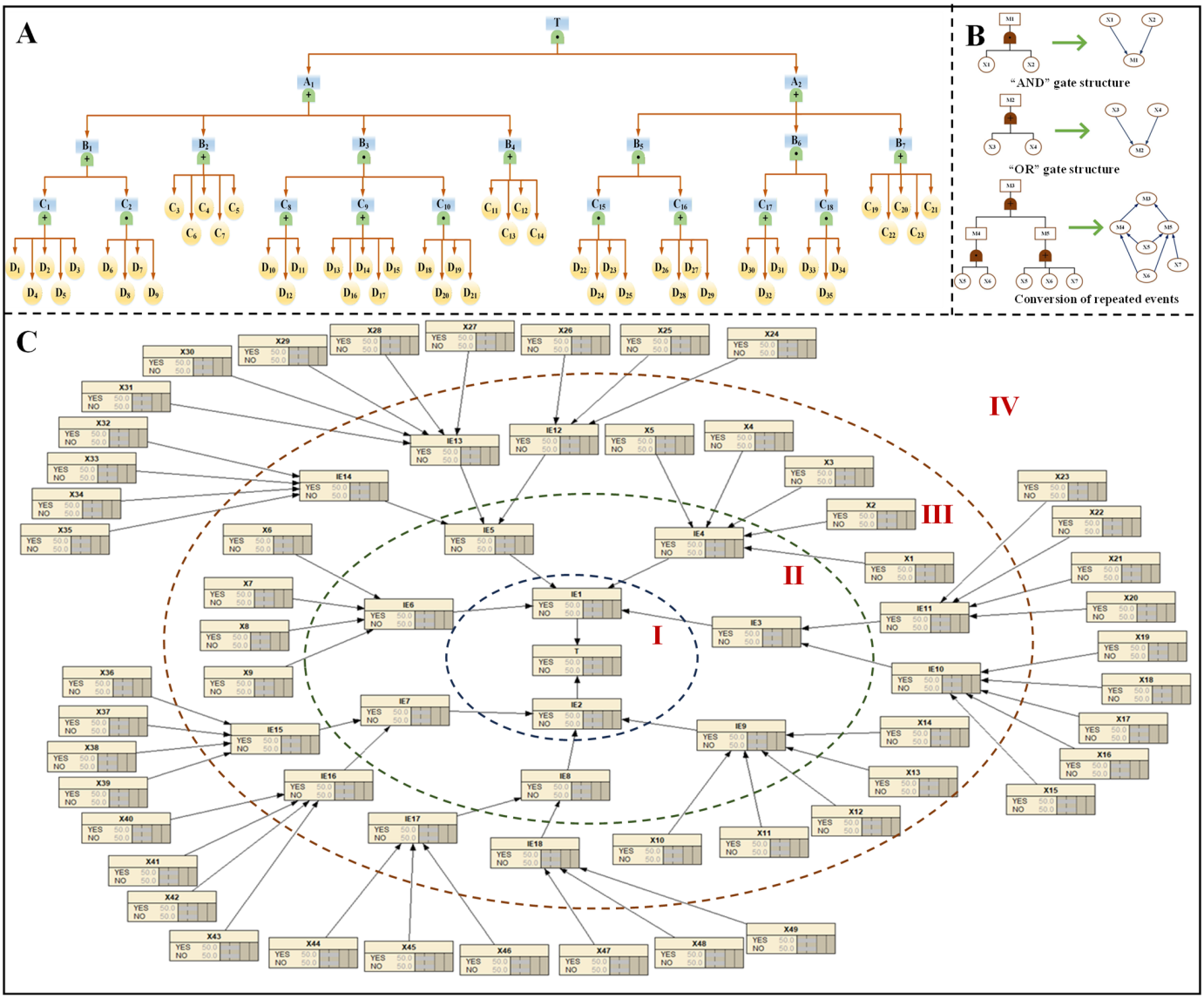


Figure 2. Model construction and conversion framework for fire risk analysis of containerized mobile power supply: (**A**) FTA model; (**B**) FTA to BN conversion rules; (**C**) BN model.

(1) Thermal runaway initiation

Mechanical damage-induced initiation was mainly sourced from dynamic loading during terminal loading, unloading, and storage operations. Dynamic loading, including hoisting impact, stacking extrusion, and wind-induced container resonance, could cause internal structural damage of cells, such as tab micro-cracks, separator thinning, and electrode assembly displacement. The high-humidity and high-salinity port environment aggravated electrochemical corrosion at the damaged sites. This corrosion effect further elevated the occurrence probability of internal short circuit and subsequent thermal runaway.

Electrical short-circuit-induced initiation was mainly induced by the port's special environmental conditions. High-humidity salt spray could cause breakdown of battery insulation layers and abrupt changes in tab contact resistance, while yard operation vibration led to loosening of high-voltage connectors and arc discharge. Management loopholes further amplified electrical short circuit risks during temporary storage. These induced disconnected lightning protection and grounding, non-compliant temporary power lines, and irregular cable laying, all of which expanded the possibility of electrical failure.

Thermal accumulation-induced initiation originated from the inherent self-discharge heat generation risk of a full-SOC containerized mobile power supply. In the open-air terminal storage scenario, excessive environmental heat input was caused by solar radiation superimposed with the greenhouse effect of closed containers. Multiple management issues blocked the normal heat dissipation path. These issues included excessive storage density, insufficient stacking spacing, over-limit stacking height, and blocked vents, which led to continuous intensification of heat accumulation and eventual thermal runaway.

External incentive-induced initiation was closely associated with the frequency of cross operations in the terminal yard. Sparks and high-temperature residues from surrounding hot work directly ignited volatile organic compound (VOC) gases released by batteries, which induced localized TR. Thermal radiation from adjacent faulty power interruption of the emergency exhaust system caused accumulation of combustible gases, which further elevated the triggering risk of external incentives.

(2) Failure of protection and emergency response systems

Failure of built-in fire protection systems was primarily caused by power supply anomalies and component defects. An interruption in the UPS power supply during temporary storage led to the shutdown of the BMS, temperature control system, and emergency exhaust systems, which prevented early risk warning and intervention. Moreover, failures or response delays of temperature, smoke, and flammable gas sensors resulted in delayed detection of fire hazards. Leakage of extinguishing agent, jamming of valves, and defects in linkage logic also disabled the built-in fire protection system, leading to the loss of the critical window for initial fire control.

Failure of external fire protection support systems was attributed to improper site selection and inadequate configuration of the temporary storage area. Incomplete coverage of fire hydrants and incompatibility between fire connectors and the port shore-based system directly restricted the rapid access of external firefighting forces. Occupied fire passage, insufficient passage width, and lack of emergency operation platforms further hindered the implementation of on-site firefighting operations.

Failure of emergency response capability was rooted in management deficiencies during temporary storage operations. The absence of special emergency plans and insufficient training on lithium battery fire response for operators led to improper handling of incipient fires. Moreover, the lack of pre-deployed emergency supplies and the absence of a joint mechanism with port fire departments resulted in delayed emergency response and failed containment of fire spread.

After the FTA model was constructed, mapping conversion was completed in accordance with the FTA-BN conversion rules presented in Figure 2B, and the final BN structure was obtained as shown in Figure 2C. Probability calculation of the model was realized via Netica 5.18 software. This software is a widely accepted universal tool in the field of BN modeling and probabilistic reasoning, which supports forward probability calculation and reverse reasoning of multi-node complex systems, with a graphical interface to intuitively present the logical correlation between different nodes.

The converted BN model was set with four hierarchical logical structures. It contained a total of 49 root nodes, 18 intermediate nodes, and 1 leaf node, which fully matched the event system of the pre-established FTA model. Strict correspondence was established between BN nodes and FTA symbols. Root nodes corresponded to the basic event of the FTA model, while intermediate nodes and leaf nodes matched the intermediate events and top event of FTA, respectively, with the detailed correspondence of all nodes and FTA symbols listed in Table 3.

Table 3. Symbol correspondence in FTA-BN model conversion.

FTA	BN	FTA	BN	FTA	BN	FTA	BN
A1	IE1	A2	IE2	B1	IE3	B2	IE4
B3	IE5	B4	IE6	B6	IE7	B6	IE8
B7	IE9	C1	IE10	C2	IE11	C3	X1
C4	X2	C5	X3	C6	X4	C7	X5
C8	IE12	C9	IE13	C10	IE14	C11	X6
C12	X7	C13	X8	C14	X9	C15	IE15
C16	IE16	C17	IE17	C18	IE18	C19	X10
C20	X11	C21	X12	C22	X13	C23	X14
D1	X15	D2	X16	D3	X17	D4	X18
D5	X19	D6	X20	D7	X21	D8	X22
D9	X23	D10	X24	D11	X25	D12	X26
D13	X27	D14	X28	D15	X29	D16	X30
D17	X31	D18	X32	D18	X33	D20	X34
D21	X35	D22	X36	D23	X37	D24	X38
D25	X39	D26	X40	D27	X41	D28	X42
D29	X43	D30	X44	D31	X45	D32	X46
D33	X47	D34	X48	D35	X49		

4. Discussion

4.1. Quantitative Calculation and Sensitivity Analysis Based on BN

Prior probabilities of each root node were comprehensively determined. Two types of supporting bases were adopted for the determination process, including publicly available similar accident cases and expert evaluation results. Preliminary probability assignment was completed for root nodes clearly involved in the cases. This assignment was implemented through a systematic case review, which restored the complete evolution process of each fire accident. Supplementary evaluation was conducted for root nodes not covered by accident cases. This part of the evaluation was completed by invited industry experts and university researchers in the field of port safety and battery fire risk control.

The Delphi method was employed for this expert probability estimation. Characterized by anonymous independent inquiry and iterative opinion collation, the approach mitigated group conformity effects and subjective bias in collective deliberation. It was well applicable to quantitative probability evaluation of complex risk factors in engineering safety, and integrated practical experience with professional theories to reach an objective consensus. A total of 20 experts and scholars were invited to participate in the evaluation, which was divided into four professional groups with equal numbers. Each group covered a core dimension of the research scenario. The groups included five front-line operators, five on-site managers of port enterprises, five port safety supervisors, and five researchers from universities and research institutes. A comprehensive evaluation of root node occurrence probability was completed. The evaluation was conducted from four perspectives: on-site operation, enterprise management, government supervision, and theoretical research, ensuring the comprehensiveness and rationality of the results.

The full implementation of the Delphi method proceeded sequentially in three stages.

In the first stage, experts were invited to review the coverage of hazard-inducing factors and the rationality of logical relationships in the FTA model. Modification suggestions were collected in this stage. Targeted optimization and improvement of the FTA model were completed based on the feedback from experts.

In the second stage, a rationality review of the preliminary probability assignment was conducted. Assignment results with large deviations were revised and adjusted through a collective review of experts, ensuring consistency with actual accident characteristics.

In the third stage, holistic probability assignment was completed. Experts were invited to conduct a comprehensive assignment of occurrence probability for all root nodes, forming a complete prior probability database for the BN model.

Differences in industry background, theoretical accumulation, and on-site familiarity existed among experts. Differentiated weights were set for the assignment results of distinct expert groups to ensure the results were consistent with the actual operation scenario of ports. The detailed weight settings are presented in Table 4. It should be noted that the risk assessment targeted port temporary storage scenarios. Front-line operators and on-site managers of port enterprises boasted abundant on-site experiences, offering a higher reference value for scenario-based risk judgement, with a unified weight of 0.286 allocated to both groups. Port safety supervisors delivered evaluations from the regulatory governance dimension, while researchers performed analysis grounded in professional theories. A uniform weight of 0.214 was adopted for the other two cohorts after overall comprehensive deliberation.

Table 4. Differentiated weight assignment for expert evaluation via the Delphi method.

Expert Category	Assigned Weight
Front-line operators	0.286
On-site managers of port enterprises	0.286
Port safety supervisors	0.214
University and research institute researchers	0.214

Meanwhile, the Cronbach's Alpha coefficient method was adopted to test the consistency of expert assignment results, with abnormal data eliminated during the test process. The relevant calculation formula is shown in Equation1. When the calculation result exceeded the preset threshold of 0.85, the expert assignment for the corresponding root node was recognized as reaching a consensus, and the corresponding prior probability was deemed valid.

$$\beta = \frac{K\left(\sigma^2 X - \sum_{i=1}^{K} \sigma^2 Y\right)}{\sigma^2 X(K-1)} \quad (1)$$

where β denotes the Cronbach's alpha coefficient; $\sigma^2 X$ represents the variance of scoring results across all root nodes; $\sigma^2 Y$ stands for the variance of scoring results for a specific root node; K is the number of root nodes.

The application scenario was set as Shenzhen Port, China. As a core cluster of China's lithium battery industry, Shenzhen maintained a high annual growth in lithium battery export volume, with the total export value of lithium batteries reaching 84.78 billion RMB in 2025, representing a year-on-year increase of 30.2%. Shenzhen Port was established as a key hub port for the export of new energy goods such as lithium batteries and new energy vehicles. The expert evaluation was conducted in combination with the operational characteristics and scenario features of Shenzhen Port. The final prior probability assignment results for each root node were illustrated in Figure 3.

Based on the expert assignment results and quantitative calculation of BN, the occurrence probability of the top event T (fire accident of containerized mobile power supply) was calculated as 2.41%. The overall fire occurrence probability remained at a low level, but a clear hazard potential was still identified.

The first level under the top event included two intermediate nodes. The occurrence probability of thermal runaway initiation IE1 was 15.0%, and the probability of failure of protection and emergency response systems IE2 was 8.08%, with the former being 1.86 times the latter. It was thus evident that TR served as a prerequisite for fire accidents. Despite the higher integration level of containerized power supply and the more sophisticated built-in

monitoring and control systems, the intrinsic risk of full-SOC cells and the failure risk of complex electrical circuits maintained the thermal runaway occurrence probability at a relatively high level. Although the occurrence probability of protection and emergency response failure was lower, it was a direct influencing factor for the evolution of thermal runaway into large-scale chain fires.

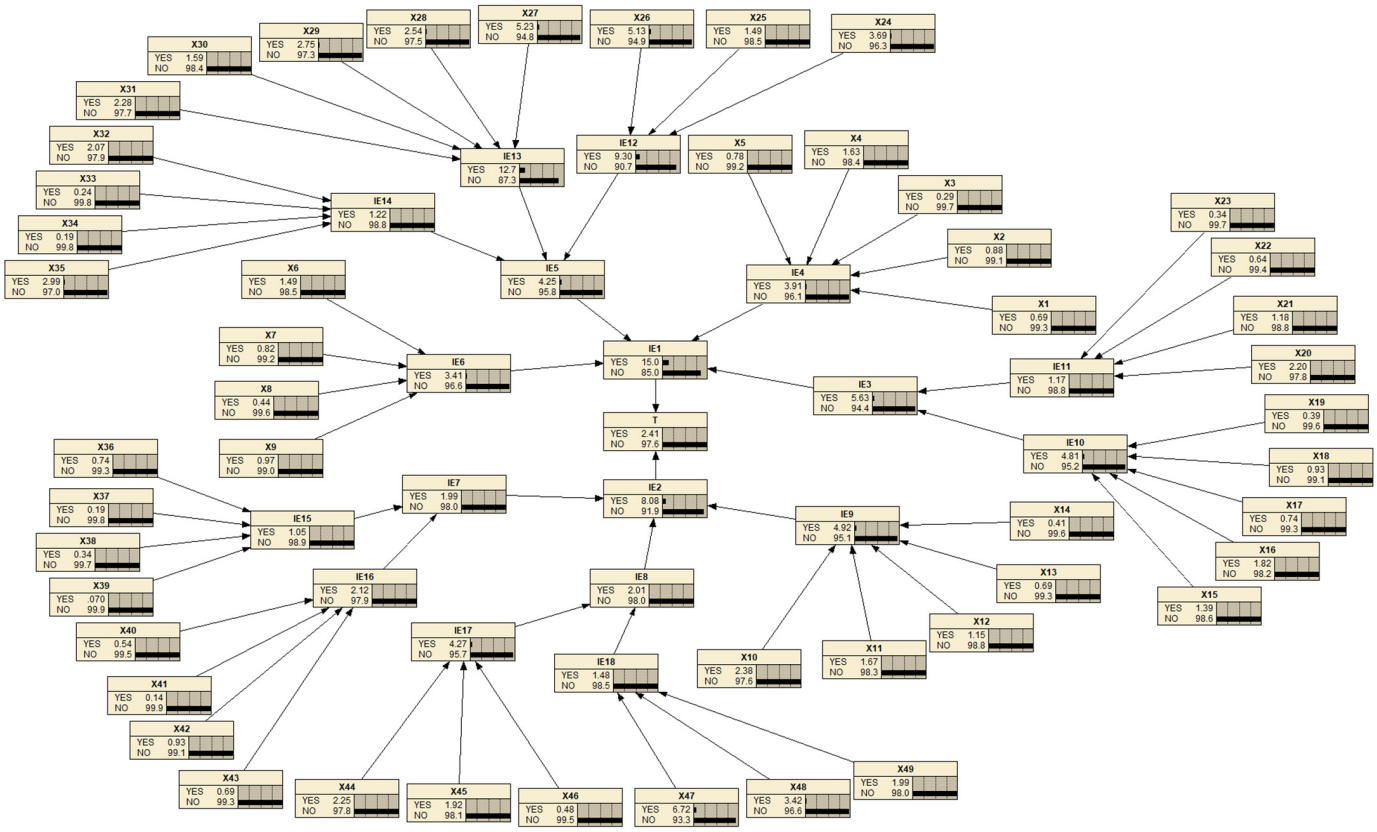


Figure 3. Occurrence probability for fire risk of containerized mobile power supply based on expert evaluation and BN calculation.

The above forward probability calculation could only clarify the overall fire risk level and hierarchical causal logic. It failed to quantify the influence of distinct root nodes on the top event. To address this limitation, the reverse reasoning capability of the BN was utilized. Posterior probability calculation was completed by setting the top event fire as an inevitable occurrence (T = 1). On this basis, sensitivity analysis was carried out to quantify the impact of single-node probability fluctuations on the top event. The sensitivity analysis focused on the second-level intermediate nodes. The posterior probability results under the condition of inevitable fire occurrence are shown in Figure 4A, and the sensitivity ranking results of each node are presented in Figure 4B.

Figure 4B illustrates that IE1 contained four intermediate nodes, which were ranked in descending order of sensitively as follows: IE3 mechanical damage-induced initiation (34.9%), IE5 thermal accumulation-induced initiation (26.3%), IE4 electrical short-circuit-induced initiation (24.3%), and IE6 external incentive-induced initiation (21.2%). Mechanical damage-induced initiation had the highest sensitivity in the temporary port storage scenario, which was relatively consistent with the results by Liu et al. [5]. The maximum sensitivity difference among the remaining three nodes was less than 5.2%, indicating an overall small gap.

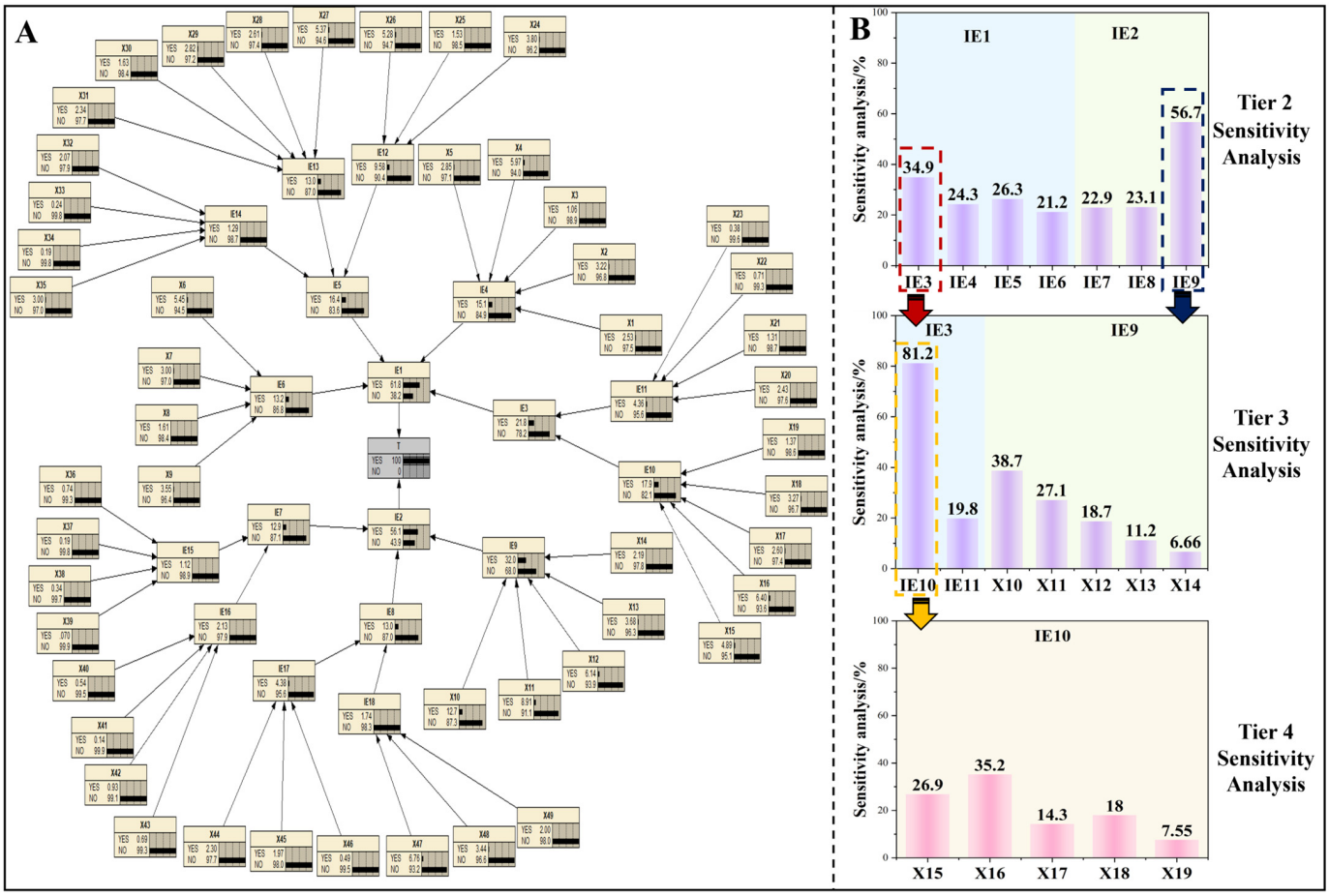


Figure 4. Posterior probability and multi-level sensitivity analysis of BN model for fire risk: (**A**) node posterior probability under inevitable occurrence of top event; (**B**) sensitivity ranking result of hierarchical nodes.

Three intermediate nodes were included in IE2. The sensitivity of IE9 failure of emergency response capability reached 56.7%, which was more than 2.4 times that of IE7 failure of built-in fire protection systems (22.9%) and IE8 failure of external fire protection support systems (23.1%). This was directly correlated with the cargo features of containerized mobile power supplies. The short temporary storage cycle and high turnover frequency of such cargoes led to the general absence of special emergency plans in ports, and operators could not apply the emergency disposal schemes for conventional lithium batteries and new energy vehicles, which easily caused fire spread due to improper disposal.

A third-level sensitivity analysis was completed through further downward disassembly. This analysis was revealed for the two nodes with the highest sensitivity, IE3 and IE9, to quantify the contribution of underlying risk factors. Among the nodes under IE3, the sensitivity of IE10 dynamic load-induced damage was more than four times that of IE11 damage–corrosion coupling-induced initiation, which was identifies as the main sources of mechanical damage. All nodes corresponding to IE9 were root nodes. These nodes matched the basic events of the FTA model, among which X10 absence of special emergency plans for temporary storage had the highest sensitivity of 38.7%. The sensitivity of X11, X12, X13, and X14, was 27.1%, 18.7%, 11.2%, and 6.66%, respectively, showing a clear downward trend.

Due to those nodes under IE9 attributed as the bottom basic event, no further downward disassembly could be conducted. A fourth-level sensitivity analysis was carried out

only targeting IE10. The five included root nodes were ranked in descending order of sensitivity as X16 (35.2%), X15 (26.9%), X18 (18.0%), X17 (14.3%), and X19 (7.55%).

In summary, sensitivity analysis based on Bayesian posterior probabilities progressively pinpointed two critical root nodes dominating the top fire event: X16 (tab microcracking and bracket plastic deformation induced by hoisting impact), and X10 (absence of special emergency plans for temporary storage). The results were consistent with the main causes of two publicly reported fire accidents (Port of Karachi in January 2026 and Port of Los Angeles in November 2025), which further verified the reliability of the posterior probability calculation results.

4.2. Identification of Critical Risk Paths and Corresponding Countermeasures

BN could only complete the sensitivity ranking of individual root nodes. It failed to account for the quantitative comparison of occurrence probabilities among distinct complete risk paths, which was a key limitation of single-node sensitivity analysis. The attack–defense game theory and the Nash equilibrium principle were introduced to address this limitation. Combined with the traversal method, the calculation and ranking of all potential risk paths were conducted systematically.

Two corresponding subjects were defined in the analytical framework of the attack–defense game. The first subject was fire hazard-inducing factors, which corresponded to the attacker with the goal of triggering the top event along the risk path. The second subject was the existing port risk prevention and control measures. This subject corresponded to the defender, whose core goal was to block the propagation of risk paths and avoid fire accidents. The Nash equilibrium principle was applied to locate the stable game state of both parties. The risk path corresponding to this state was identified as the path with the highest occurrence probability and the greatest prevention and control difficulty.

The specific calculation process was divided into three sequential steps. Each step was designed in strict accordance with the logical rules of FTA and BN models established in the previous research.

The first step was basic parameter assignment. According to the occurrence probability of each root node obtained from the previous expert evaluation, the probability transfer rules of hierarchical nodes were clarified in strict compliance with the logic gate rules of the FTA model.

The second step was full-path traversal and probability calculation. The traversal method was employed to identify all effective risk paths that could trigger the top event, and the occurrence probability of each complete path was calculated based on the established probability transfer rules.

The third step was path ranking and screening. Formed on the full-path probability calculation results, all paths were ranked in descending order of occurrence probability, and the high-probability critical risk paths were identified.

The critical risk evolution paths of fire accidents for containerized mobile power supply in temporary port storage were finally obtained, with the corresponding results presented in Figure 5 and Table 5.

IE1 and IE2 conformed to AND gate logic and acted as two independent prerequisites for activating the top fire event. In the analysis of key risk evolution trajectories, simultaneous consideration of IE1 and IE2 was restricted by the low baseline accident probability in risk assessment. Superimposed computation further lowered the occurrence likelihood of key trajectories and rendered them meaningless for horizontal comparative analysis. Accordingly, IE1 and IE2 were respectively defined as the terminal nodes of key risk evolution trajectories. Grounded in attack–defense game theory, the traversal algorithm was employed to clarify the evolutionary rules of such risk trajectories. The root

nodes obtained from the two finalized trajectories matched perfectly with the dominant root nodes affecting the top fire event in sensitivity analysis, which further validated the credibility of the analytical findings.

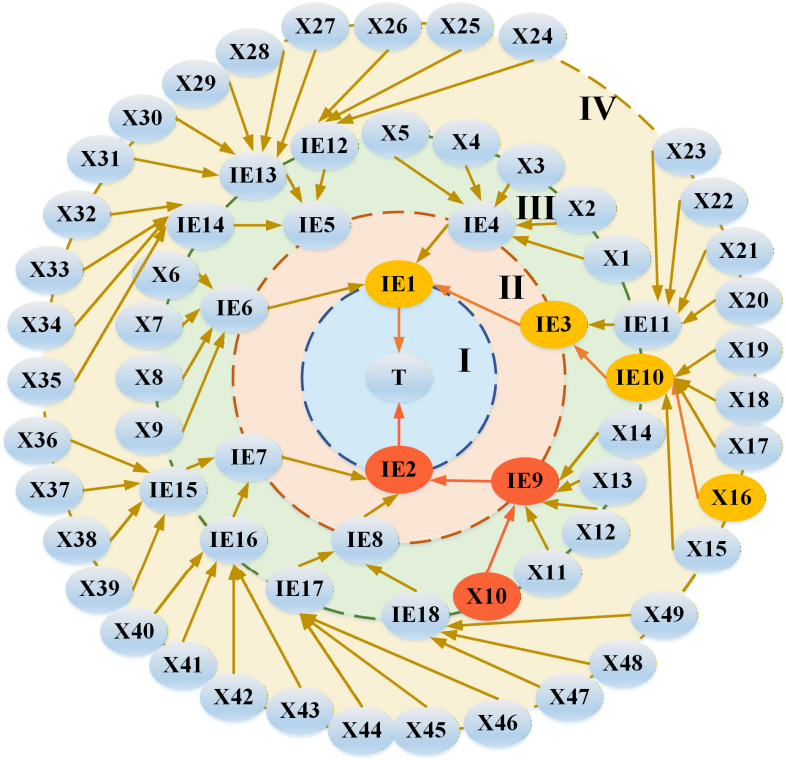


Figure 5. Critical risk evolution paths concerning containerized mobile power supplies.

Table 5. Critical risk evolution paths and occurrence probabilities.

Root node	Evolution Path	Occurrence Probability
X16 tab micro-cracking and bracket plastic deformation induced by hoisting impact	X16-IE10 dynamic load-induced damage; IE3 mechanical damage-induced initiation; IE1 thermal runaway initiation	1.50%
X10 absence of special emergency plans for temporary storage	X10-IE9 failure of emergency response capability; IE2 failure of protection and emergency response systems	1.77%

The evolution chain of the first path was defined as follows: X16-IE10-IE3-IE1, with an occurrence probability of 1.50%. Mobile power supplies were kept at a full-SOC upon port entry. The cells themselves were in a high energy storage state, which resulted in a lower triggering threshold for internal short circuit. Yard storage of such cargoes was only set as a transit link with a fast turnover rhythm. The hoisting operation window was compressed by ports to match shipping schedules, and impact loads caused by sudden stops, sudden releases, and alignment deviations were generated during the only two hoisting operations for yard entry and exit. The potential of such impact loads could induce cell tab micro-cracks and plastic deformation of internal support structures These damages were classified as internal hidden defects, which could not be identified through the conventional appearance inspection implemented at ports.

Further limitations on risk detection were brought by the transit attribute of temporary storage. No standing period and refined internal resistance detection window, which were routine procedures for conventional lithium battery cargoes, were provided for such goods

during temporary storage. Unidentified defects were continuously developed, and an internal short circuit of cells was induced. Dynamic load damage was formed through this process, and mechanical damage-related thermal runaway was eventually triggered. The high-temperature and high-humidity environment of the open port yard accelerated the internal side reactions of full-SOC cells. It also sped up the heat generation process of internal short circuit, which compressed the time interval from defect generation to thermal runaway triggering and enabled the whole conduction process to be completed within the temporary storage period.

Thermal runaway served as the initial prerequisite for fire occurrence. Failure of protection and emergency response was identified as the direct cause for the evolution of incipient fire into large-scale accidents, which determined the final severity of the fire event. The second path was defined as follows: X10-IE9-IE2, with an occurrence probability of 1.77%.

Such cargoes were classified as non-standard temporary transit goods in port yards. Their storage location and cycle were dynamically adjusted with shipping schedules, which meant they were not included in the routine normalized management and control system for hazardous chemicals in ports. No targeted special emergency plan was formulated for such cargoes. The plan development failed to cover their integrated closed structure and full-SOC thermal runaway characteristics, leaving a critical gap in port emergency management. Yard operators and emergency disposal personnel were unfamiliar with the fire evolution law of such containers. Conventional disposal procedures for standard lithium batteries and new energy vehicles were completely inapplicable to thermal runaway fires inside closed containers, which greatly increased the risk of improper emergency operations.

The wind environment in open port yards accelerated risk propagation after thermal runaway occurrence. It promoted the accumulation of combustible gases and fire spread inside the container, and disposal personnel easily missed the critical initial fire control window without special disposal guidelines. Improper disposal directly led to the failure of emergency response capacity. It further triggered the comprehensive failure of the entire protection and emergency system, resulting in the eventual large-scale fire accident. Similar fire accidents were recorded in two international hub ports. These accidents occurred at the Port of Karachi in January 2026 and the Port of Los Angeles in November 2025, where rapid incipient fire expansion was caused by the absence of special emergency plans and mismatched disposal procedures. The evolution logic of these accidents was highly consistent. It matched the risk evolution path sorted out in this study, which further verified the reliability of the path identification results.

The initiation mechanisms of the two core risk evolution paths corresponded separately to physical hazard risks in operational procedures and systematic failure risks in management modules, requiring the formulation of targeted regulatory measures. For the thermal runaway path, defined as the key risk evolution path terminating at IE1, risk regulation was conducted from three primary perspectives.

First, the coordination between hoisting operations and shipping schedules was optimized to avoid irregular operations caused by operation time compression for schedule compliance, and specific requirements for hoisting lifting/lowering speed and alignment accuracy were clarified to reduce the risk of cell damage induced by impact loads. Second, a rapid inspection procedure for yard entry was established. Infrared thermal imaging and portable internal resistance sampling inspection were adopted to complete the preliminary screening of hidden defects in incoming cargoes, which fully adapted to the operation characteristics of short-cycle storage. Third, fixed special storage areas were designated. Locations with favorable sunshade and ventilation conditions were preferentially

selected to mitigate the continuous adverse impact of high-temperature and high-humidity environments on battery cells.

For the failure path of protection and emergency response, which reflected the initiation mechanism of the critical risk evolution path terminating at IE2, risk governance centered on the optimization of the safety management system.

Management and control for the protection and emergency response failure path focused on the improvement of the management system. Three targeted optimization measures were formulated, covering the full chain of system construction, personnel training, and on-site emergency support. First, special management and control regulations and emergency plans were compiled. The demarcation of storage locations, operation requirements, and phased fire disposal procedures for temporary storage were clearly defined, and the direct application of management requirements for conventional lithium batteries was prohibited. Second, special training sessions were carried out. The training covered personnel in all links, including hoisting, yard management, and emergency disposal, with a focus on explaining the structural characteristics of containerized power supplies and the key disposal points for fires in closed containers. Third, corresponding emergency supplies were equipped in the special storage areas. The response procedure for incipient fires was clearly specified to shorten the emergency disposal response time.

5. Conclusions

This study focused on the fire risk of containerized mobile power supplies during temporary storage at ports. FTA, BN, and attack–defense game theory were integrated to complete qualitative identification and quantitative analysis of accident causes, clarify critical risk evolution paths, and formulate corresponding management and control requirements. The main research achievements are summarized as follows:

(1) Similar fire accident cases were collected and analyzed. Combined with the unique scenario characteristics of containerized mobile power supplies in a port yard, including full stage of charge, temporary storage nature, and high turnover frequency, hazard-inducing factors across the full chain of fire accidents were systematically identified. A complete FTA model was constructed, and the causal logic of the accident from underlying incentives to the occurrence of the top event was clarified.

(2) A BN model for fire risk assessment was established, which contained 4 logical levels, 49 root nodes, 18 intermediate nodes, and 1 leaf node. Quantitative calculation was performed according to the expert evaluation results, and the occurrence probability of fire accidents at the target port was determined as 2.41%. Two root nodes with the most significant impact on the top event were identified: X10 absence of special emergency plans for temporary storage, and X16 tab micro-cracking and bracket plastic deformation induced by hoisting impact.

(3) The attack–defense game theory, combined with the traversal method, was employed for risk path identification. Two critical risk evolution paths were sorted out and verified, with occurrence probabilities of 1.50% and 1.77%. The triggering logic of each path was disassembled in combination with the features of the port temporary storage scenario, and targeted management and control requirements for each link were proposed, corresponding to the risk evolution characteristics of the two paths.

The research outcomes laid a theoretical basis for fire hazard causation identification and quantitative risk assessment of mobile power units in temporary port storage. Furthermore, quantitative results from on-site operational scenarios supported the formulation of targeted risk mitigation schemes for vulnerable segments of different ports, facilitating the improvement of safety management proficiency among port operators.

Subsequent research will broaden the coverage of industry expert consultation and expand the panel of participating specialists. Updated accident statistics and typical case records will be incorporated in a timely manner to solidify the foundational framework of risk analysis and evaluation. Furthermore, attack–defense game theory will be adopted to further polish the proposed risk control countermeasures, rationalize the allocation of preventive resources, clarify the risk reduction probability, and enhance the implementation efficiency and practical application value of these countermeasures.

Author Contributions: Data curation, Z.Q., X.Z., Y.T., Y.Z. (Yamei Zeng), W.C., Y.M., and Y.Z. (Yuechao Zhao); methodology, Z.Q., Y.G., and L.H.; visualization, Z.Q. and X.Z.; writing—original draft, Z.Q.; writing—review and editing, Z.Q., X.Z., Y.G., and Y.T. All authors have read and agreed to the published version of the manuscript.

Funding: This research was funded by Basic Scientific Research Operating Expenses Project of China Waterborne Transport Research Institute, grant number 42503, 42602.

Institutional Review Board Statement: Not applicable.

Informed Consent Statement: Not applicable.

Data Availability Statement: All data generated or analyzed during this study are included in this published article.

Acknowledgments: The authors have reviewed and edited the output and take full responsibility for the content of this publication.

Conflicts of Interest: The authors declare no conflicts of interest.

References

1. Ganjian, M.; Farahabadi, H.B.; Firuzjaei, M.R. Voyage scheduling and energy management co-optimization in hydrogen-powered ships. *Int. J. Hydrogen Energy* **2024**, *86*, 788–799. [CrossRef]
2. Perčić, M.; Ančić, I.; Vladimir, N. Life-cycle cost assessments of different power system configurations to reduce the carbon footprint in the Croatian short-sea shipping sector. *Renew. Sustain. Energy Rev.* **2020**, *131*, 110028. [CrossRef]
3. Paipa-Sanabria, E.; González-Montoya, D.; Coronado-Hernández, J.R. Green technologies for environmental air and water impact reduction in ships: A systematic literature review. *J. Mar. Sci. Eng.* **2025**, *13*, 839. [CrossRef]
4. Frković, L.; Ćosić, B.; Pukšec, T.; Vladimir, N. Vehicle-to-Ship: Enhancing the energy transition of maritime transport with the synergy of all-electric vehicles and ferries. *IEEE Trans. Transp. Electrif.* **2024**, *10*, 6010–6023. [CrossRef]
5. Liu, J.; Zhu, D.; Yuan, D.Y.; Yao, J. FMEA-based assessment of the battery swapping process in electric ships: A hybrid approach integrating fuzzy evidential reasoning and dynamic network VIKOR algorithm. *Expert Syst. Appl.* **2025**, *294*, 128811. [CrossRef]
6. Guo, S.Q.; Wang, Y.B.; Yue, M.Y.; Dai, L.; Fang, S.; Zhang, S.; Hu, H. Optimization of energy replenishment for inland electric ships considering multi-technology adoption and partial replenishment. *J. Mar. Sci. Eng.* **2025**, *13*, 2092. [CrossRef]
7. *JT/T 1543-2025*; Safety technical requirements for the transport of lithium batteries by ships. China Communications Press Co., Ltd.: Beijing, China, 2025.
8. Meng, X.D.; Yang, K.; Zhang, M.J.; Gao, F.; Liu, Y.; Duan, Q.; Wang, Q. Experimental study on combustion behavior and fire extinguishing of lithium iron phosphate battery. *J. Energy Storage* **2020**, *30*, 101532. [CrossRef]
9. Zhou, Z.Z.; Zhou, X.D.; Peng, Y.; Li, L.; Cao, J.; Yang, L.; Cao, B. Quantitative study on the thermal failure features of lithium iron phosphate batteries under varied heating powers. *Appl. Therm. Eng.* **2021**, *185*, 116346. [CrossRef]
10. Wang, J.L.; Yang, J.J.; Bai, W.; Wang, Z.; Yu, K.; Lu, Y.; Han, C. Thermal runaway and jet flame features of LIBs undergone high-rate charge/discharge: An investigation. *J. Energy Chem.* **2025**, *103*, 826–837. [CrossRef]
11. Frivaldsky, M.; Simcak, M.; Andriukaitis, D.; Navikas, D. Cycling operation of a LiFePO4 battery and investigation into the influence on equivalent electrical circuit elements. *Batteries* **2025**, *11*, 211. [CrossRef]
12. Wang, Y.; Lu, X.; Zhang, Y.X.; Liu, L. Thermal runaway behaviour and heat generation optimization of the marine battery cabinet based on module thermal analysis. *Appl. Therm. Eng.* **2024**, *240*, 122188. [CrossRef]
13. Jin, C.W.; Xu, J.; Jia, Z.Y.; Xie, Y.; Zhang, X.; Mei, X. Expansion force signal based rapid detection of early thermal runaway for pouch batteries. *Energy* **2024**, *312*, 133685. [CrossRef]
14. Zhang, S.G.; Zhang, R.X.; Tan, T.F.; Liu, J.; Liu, J.; Wang, J.; Li, Q.; Cong, B. Characteristics of gas explosion caused by lithium-ion battery thermal runaway in a prefabricated cabin of energy storage station. *Fire Technol.* **2026**, *62*, 23. [CrossRef]

15. Schoberl, J.; Wong, S.K.; Kroner, T.; Klein, N.; Liu, X.; Bilfinger, P.; Xia, Y.; Zhang, F.; Grosu, C.; Feng, X.; et al. A methodology for reliable thermal runaway propagation mitigation in battery systems with large-format prismatic NMC-811 and LFP battery cells. *eTransportation* **2026**, *28*, 100564. [CrossRef]
16. Shareef, S.M.; Rao, G.A.P. Advancements in lithium-ion battery materials for thermal runaway prevention. *Electrochem. Commun.* **2026**, *182*, 108098. [CrossRef]
17. Li, H.B.; Qu, X.Y.; Pan, Y.C.; Li, N.; Zhou, C.; Zhao, Z.; Xing, Z.; Shi, X.; Tian, X.; Wang, P. Customized design of LiF-Rich SEI layer on lithium metal anode for high flame retardant electrolyte. *Carbon Energy* **2025**, *7*, e70077. [CrossRef]
18. Yang, L.; Yang, J.Z.; Fan, A.L.; Zhou, R.; Wang, L. Fire risk assessment of electric ships on inland waterway based on GT-FFTA: A case study of China. *Ocean. Eng.* **2025**, *332*, 121329. [CrossRef]
19. Yin, R.; Du, M.; Shi, F.L.; Cao, Z. Risk analysis for marine transport and power applications of lithium ion batteries: A review. *Process Saf. Environ. Prot.* **2023**, *181*, 266–293. [CrossRef]
20. Lee, J.; Park, S.K.; Bazher, S.A.; Seo, D. Development of a fault prediction algorithm for marine propulsion energy storage system. *Energies* **2025**, *18*, 1687. [CrossRef]
21. Guo, C.Q.; Utne, I.B.; Zadeh, M. Real-time risk monitoring of autonomous all-electric ships' battery systems based on risk indicator data. *J. Mar. Eng. Technol.* **2025**, *24*, 228–240. [CrossRef]
22. Qiao, Z.; Zhan, X.T.; Tian, Y.; Gao, Y.; He, L.; Lu, Y. Fire risk assessment of lithium-ion power battery shipping containers in maritime transportation scenarios. *Fire* **2025**, *8*, 453. [CrossRef]
23. Andrews, J. Evaluating minimal cut sets and the Fussell-Vesely measure of component importance using the Dynamic and Dependant Tree Theory methodology. *Reliab. Eng. Syst. Saf.* **2026**, *272*, 112561. [CrossRef]
24. Popa, C.; Stefanov, O.; Goia, I.; Nistor, F. A hybrid fault tree-fuzzy logic model for risk analysis in multimodal freight transport. *Systems* **2025**, *13*, 429. [CrossRef]
25. Kabir, S.; Papadopoulos, Y. Applications of Bayesian networks and Petri nets in safety, reliability, and risk assessments: A review. *Saf. Sci.* **2019**, *115*, 154–175. [CrossRef]
26. Marcot, B.G.; Penman, T.D. Advances in Bayesian network modelling: Integration of modelling technologies. *Environ. Model. Softw.* **2019**, *111*, 386–393. [CrossRef]
27. Hosseini, S.; Ivanov, D. Bayesian networks for supply chain risk, resilience and ripple effect analysis: A literature review. *Expert Syst. Appl.* **2020**, *161*, 113649. [CrossRef] [PubMed]
28. Gao, Y.; Qiao, Z.; He, L.J. Systematic risk assessment of seawater intrusion in ports: Assessment framework and empirical analysis. *Systems* **2026**, *14*, 160. [CrossRef]
29. Tsadikovich, D.; Levner, E. Integrating attack-defense graphs with online control to enhance cybersecurity of smart university campuses. *Control Eng. Pract.* **2026**, *173*, 107006. [CrossRef]
30. Yoon, H.J.; Thukkaraju, A.R.; Matsumoto, S.; Ferrari, J.F.; Lee, D.; Ahn, M.K.; Costa, P.; Cho, J.-H. Subjective-Bayesian-Network-Based interdependent mission impact assessment with Game-Theoretic Attack-Defense interactions. *IEEE Internet Things J.* **2025**, *12*, 6548–6562. [CrossRef]

Disclaimer/Publisher's Note: The statements, opinions and data contained in all publications are solely those of the individual author(s) and contributor(s) and not of MDPI and/or the editor(s). MDPI and/or the editor(s) disclaim responsibility for any injury to people or property resulting from any ideas, methods, instructions or products referred to in the content.